# A compact fiber-laser-based system for detection of biological agents via coherent Raman spectroscopy

N. Coluccelli*[a], G. Cerullo[a], P. Laporta[a], K. Curtis[b], K. McEwan[b], C. R. Howle[b],
[a]Dipartimento di Fisica, Politecnico di Milano, Piazza Leonardo da Vinci, 32, 20132 Milano Italy
[b]Defence Science and Technology Laboratory, Porton Down, Salisbury SP4 0JQ, UK

## ABSTRACT

We report on a compact laser system for detection of hazardous biological agents by standoff coherent anti-Stokes Raman spectroscopy (CARS). The system is based on ytterbium-laser technology featuring broad spectral coverage and high-sensitivity. High-quality CARS spectra have been obtained for NaDPA powder, a substitute for CaDPA, which is the Raman marker of bacterial spores. In addition, endospores of *B. atrophaeus* deposited over a glass substrate have been detected by their CARS signature at a standoff distance of 1 m and an integration time of 1 s. The system will be further developed for imaging of bacterial spores deposited over wide surface areas at standoff distances.

**Keywords:** Biological Warfare Agents, Coherent Raman Spectroscopy, Ytterbium Lasers, Optical Parametric Amplifiers.

## 1. INTRODUCTION

Worldwide, the risk of chemical and biological attacks on populations is of growing concern. It is vital to have an integrated device allowing for fast and reliable monitoring of relevant resources, infrastructures, and processes to reduce vulnerabilities and ultimately the overall risk for populations. For this purpose, we developed a standoff CARS system based on ytterbium laser technology with broad spectral coverage and high-sensitivity allowing for clear detection of bacterial spores. Coherent Raman spectroscopy has been widely recognized as a tool for observation of molecular vibrations, providing identification of chemical species in many different fields [1]. In this context, broadband coherent anti-Stokes Raman scattering spectroscopy is very attractive, as it combines the acquisition speed enabled by the coherent excitation with the multispectral information capability that is required for molecular fingerprinting. Among the several CARS detection techniques reported so far [2-7], hybrid-CARS [8,9] has been used as a time domain technique featuring strong non-resonant background rejection, resolution limited by the linewidth of the probe pulse, and broadband acquisition. The relevant hybrid-CARS systems reported so far are based on bulk Ti:sapphire lasers to take advantage of the broadband pulses with typical energy of 1-10 μJ and Raman spectral span of 500-1800 $cm^{-1}$. In this paper, we report on a hybrid-CARS spectroscopy system based on using a single high-energy ytterbium laser source coupled to an Optical Parametric Amplifier (OPA), enabling measurement of CARS spectra with exceptionally high sensitivity and maximum Raman shifts of 2000 $cm^{-1}$. In particular, we observed CARS spectra of NaDPA powder, a substitute for CaDPA, which is the Raman marker for bacterial spores, at a standoff distance of 1 m and integration time of 100 ms. In addition, we demonstrated standoff detection of *B. atrophaeus* spores by observation of their characteristic Raman resonances at 1017, 1390, 1445, 1570 $cm^{-1}$; the spore sample was deposited on a glass surface at a distance of 1 m from the laser system and the integration time was set to 1 s. The system will be further developed for fast imaging of bacterial spores deposited over wide surfaces at standoff distance.

## 2. EXPERIMETAL SETUP

### 2.1 Principle of operation of hybrid CARS

In the frequency domain, the pump and Stokes pulses are broadband pulses exciting coherent vibrations of molecules within the target; the range of Raman vibrations excited depends on the bandwidth of the pump and Stokes pulses. A narrow band probe pulse is frequency shifted by the molecular vibrations excited within the target and backscattered (Figure 1). The band of the probe pulse determines the final resolution of the measurement, that is the minimum width of spectral lines observed in the backscattered Raman spectrum. Each Raman vibration shifts the probe frequency by an

amount corresponding to the frequency of the Raman vibration considered, with a resulting one-to-one mapping of all Raman active vibrations to higher optical frequency, which can be detected by a single parallel measurement using a spectrometer. The technique is inherently broadband and fast. In the time domain, the pump and Stokes pulses are ultrashort pulses with typical durations of tens of femtoseconds which can be viewed as the preparation pulses. A time delayed probe pulse with typical duration of around 1 ps probes the vibrational coherence excited within the target sample by the preparation pulses. The ultrashort pump and Stokes pulses excite all vibrational states of the target overlapped by the bandwidth of the pulses. The probe laser beam, with a much narrower bandwidth, scatters off this coherence to produce a fourth beam which is blue-shifted from the probe by the frequency of the resonances.

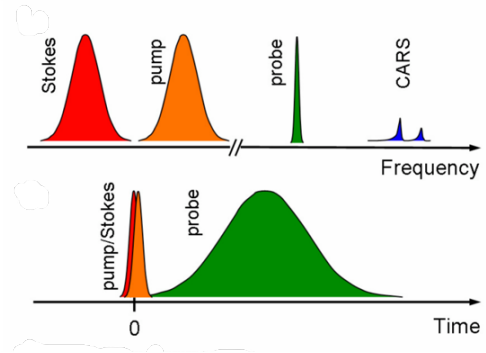


Figure 1. The principle of operation of hybrid-CARS

## 2.2 Optical system for hybrid CARS

The system is based on a compact amplified Ytterbium laser that generates 1030 nm femtosecond pulses (5-nm FWHM bandwidth) at a repetition rate tunable from 1 to 100 kHz. For all experiments, the laser was set to a pulse energy of 250 uJ, pulse duration of 250 fs, and repetition rate of 10 kHz, corresponding to an average power of 2.5 W (Figure 2). The beam at the output of the Yb-laser is focused onto a lithium triborate (LBO) nonlinear crystal for second harmonic (SH) generation at 515 nm. The SH beam at 515 nm provides the pump for the optical parametric amplification (OPA), while the residual of the fundamental beam at 1030 nm is separated from the SH beam by means of a dichroic beamsplitter and is used for the generation of a white light seeder. The SH LBO crystal provides an efficiency of around 50% so that pulse energies of around 125 uJ at 515 nm are obtained at the output. The residual pulse energy of 2 uJ at 1030 nm is focused onto a 6-mm YAG plate in order to generate the white light seed with spectral coverage from 400 to 1200 nm. The white light seed pulses and SH pulses are synchronized and focused onto a BBO crystal providing OPA; the output of the OPA provides signal pulses with energy of around 0.05 µJ, center wavelength tunable from 850 to 960 nm, and bandwidth of 50 nm, corresponding to 600 $cm^{-1}$. After first OPA interaction, the signal pulses are further amplified within two cascaded OPA stages to 14 µJ, providing the pump pulses for Hybrid-CARS; the residual of the fundamental pulses at 1030 nm, with energy content of around 100 µJ, is used as the Stokes pulses, whereas the residual of the SH pulses at 515 nm are used as the probe after spectral narrowing in a home-made pulse shaper.

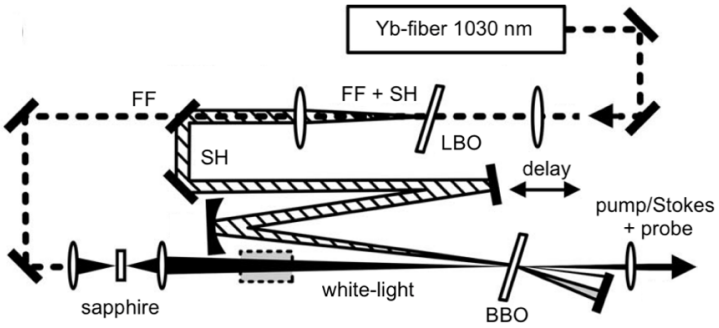


Figure 2. Layout of the OPA source

Figure 3 shows the configuration of the laser, OPA source, collection optics, and acquisition system for standoff detection at a distance of 1 m. The sample is illuminated by the three collinearly propagated laser pulses, specifically the pump, the Stokes and the probe pulses, using a lens with a focal length of 1 m. All pulses are synchronized by computer-controlled delay stages. The backscattered CARS radiation is collected by a 2-inch fused silica lens with focal length of 300 mm placed at 1 m from the sample, and coupled into the spectrometer through a fiber bundle. The CARS spectra are imaged onto a back-illuminated CCD camera with thermoelectric cooling at -50 degree Celsius. Finally, the signal is digitized and displayed by a pc-software interface.

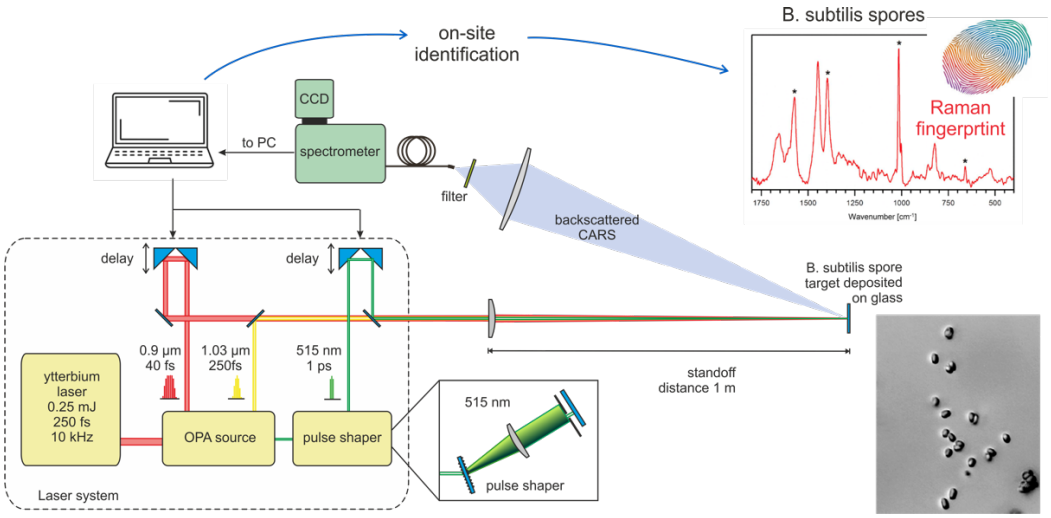


Figure 3. Layout of the system for standoff detection by hybrid CARS

## 3. MEASURMENTS OF CARS SPECTRA OF BACTERIAL SPORES

### 3.1 Hybrid-CARS results

As a first demonstration of the performance of hybrid-CARS, we measured the CARS spectrum of NaDPA powder. NaDPA is a substitute for CaDPA and is much easier to synthesize. CaDPA represents around 15% of bacterial spore weight and is considered as the main marker for detection of bacterial spores by Raman spectroscopy. Figure 4 shows the spectrograms of NaDPA powder corresponding to pump pulse wavelengths of 895, 915, 930, 945 nm. By tuning the pump pulse wavelengths while keeping fixed the Stokes pulse wavelength at 1030 nm, it is possible to tune the central frequency of the CARS spectrum and excite different resonances from 600 to 1800 $cm^{-1}$. The spectrograms are taken at a standoff distance of 1 m; the integration time of the spectrometer is set to 100 ms. The energy of the pump, Stokes, and probe pulse was set to 2, 3, 1.5 µJ, respectively, at a repetition frequency of 10 kHz. The streaked horizontal lines apparent in Fig. 4 are the signature of excited Raman transitions of NaDPA while the broadband pedestal visible at zero delay is the NR background. The resonant and NR contributions exhibit different dependencies on the probe delay. The magnitude of the NR background is determined by the overlap of the three laser pulses and follows the $sinc^2$ probe pulse temporal profile; the duration of the probe pulse can be evaluated from the horizontal cross sections of the spectrogram and is found to be ~1 ps. In contrast, the streaked resonant Raman features have relatively long decay time which allows for their effective discrimination over the NR background when the probe is delayed. The absolute frequencies of the observed Raman vibrations are calculated as the frequency separation of the retrieved peaks with respect to the probe. Figure 5 shows the cross-sections of the hybrid-CARS spectrograms of NaDPA powder corresponding to probe delays of 2.5 ps along with the reference spontaneous Raman spectrum as measured by state-of-the-art Raman micro-spectrometer. Using probe delays of 2.5 ps allows for optimized detection in terms of intensity ratio between the resonant and NR contributions. The main

Raman resonances of NaDPA are clearly resolved by hybrid-CARS and the corresponding frequency correctly identified. More specifically, by setting the pump pulse wavelength to 915 nm, it is possible to excite a broadband CARS response including the lines at 1004, 1082, 1153, 1187, 1390, 1445 $cm^{-1}$ which can be readily used for software-based assignment. The triplet at 1390, 1445, 1580 $cm^{-1}$ is particularly strong and could be also efficiently used for detection, as the corresponding combination of Raman frequencies is highly specific of NaDPA.

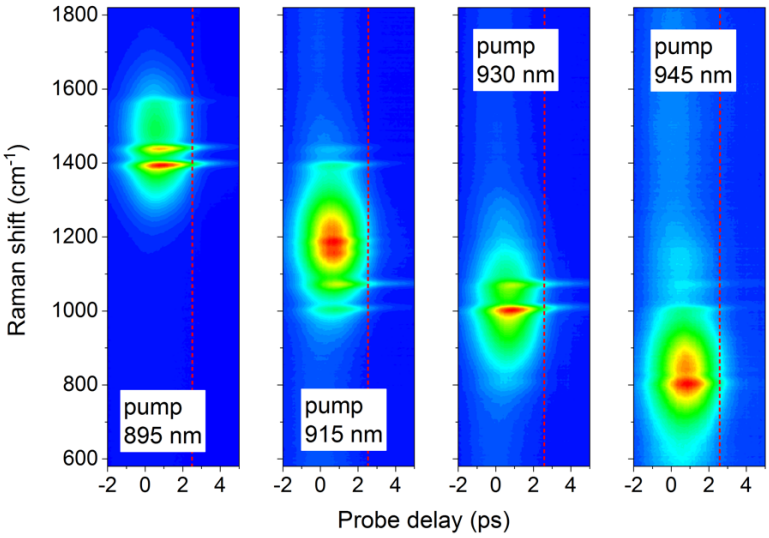


Figure 4. CARS spectrogram of NaDPA powder as measured at standoff distance of 1 m and integration time of 100 ms. The dotted lines indicate the cross-sections (spectra) corresponding to probe pulse delays of 2.5 ps, shown in Fig. 5.

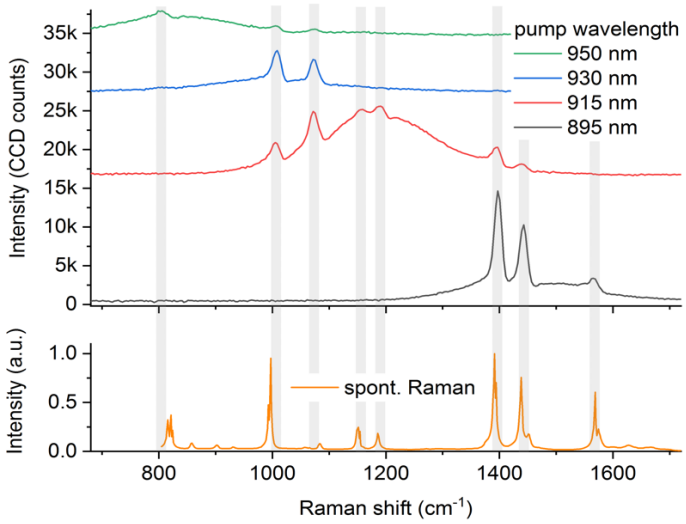


Figure 5. Cross-sections of the hybrid-CARS spectrogram of Fig. 4 taken at probe delays of 2.5 ps for NaDPA powder and reference spectrum as measured with a spontaneous Raman microscope and integration time of 30 s.

Hybrid-CARS spectra obtained on *B. atrophaeus* spores are shown in Figure 6. In this case the cross-sections have been measured at zero probe delay to take advantage of the stronger signal due to enhanced interference with the local oscillator represented by the NR background. The data are then processed to retrieve the resonant contribution. In particular, the raw data corresponding to the sum of NR background and resonant contributions have been filtered by a low-pass filter to smooth out the resonant contribution and then fitted by a Gaussian; the fitted Gaussian is subtracted from the raw data to retrieve the resonant contribution. Extracted CARS profiles are then shown in Figure 7 along with the reference Raman spectrum of *B. atrophaeus* spores as measured with a state-of-the-art Raman micro-spectrometer. The Raman band from 800 to 1700 $cm^{-1}$ is observed by setting the pump pulse wavelength at 895 and 930 nm, with a measurement time of 1 s at a distance of 1 m from the sample. The Raman lines at 1017, 1390, 1445, and 1570 $cm^{-1}$ are clearly detected and resolved. The absolute frequencies of the Raman transitions are calculated based on the relative shift from the probe wavelength; the values are in good agreement with the results of spontaneous Raman measurements. The data shown in Figure 7 are acquired with an integration time of 1 s, although the strong Raman lines stand out from the background even after 100 ms of integration.

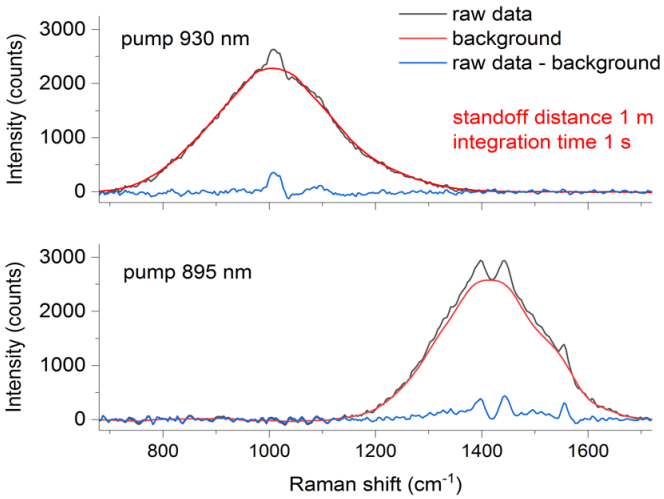


Figure 6. Cross sections of the hybrid CARS spectrogram of *B. atrophaeus* spores corresponding to a probe delay of 2.5 ps, and pump pulse wavelengths of 930 nm (top) and 895 nm (bottom). The black line represents the raw data (non-resonant background and resonant CARS), the red line is a Gaussian fit used for background removal, the blue line represents the retrieved resonant CARS contribution.

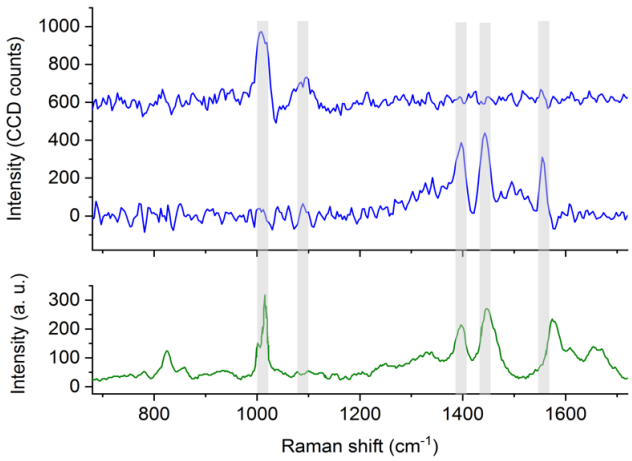


Figure 7. The CARS response of *B. atrophaeus* spores as measured with hybrid-CARS setup at standoff distance of 1 m, integration time of 1 s, and pump pulse wavelengths of 930 and 895 nm (top and bottom blue line, respectively) along with the reference spontaneous Raman spectrum (green line).

## 4. CONCLUSION

In conclusion, a hybrid-CARS spectrometer with broad spectral coverage and sensitivity has been demonstrated using a high-energy Yb-laser and OPA source. High-quality CARS spectra of *B. atrophaeus* have been measured in the Raman range from 1000 to 1600 $cm^{-1}$, with an observation time of 1 s. The system is currently under revision to improve the spectral coverage of Raman frequencies so that the whole band from 1000 to 1600 $cm^{-1}$ can be observed at the same time; this will provide at least a set of four strong Raman lines for fast and confident detection. A systematic study of the damage threshold as a function of pulse energies of the pump, Stokes, and probe, will allow for optimization of the signal-to-noise ratio of the measurement. Being based upon compact, robust ytterbium laser technology, the system could be applied to onsite detection of hazardous biological agents.


### ACKNOWLEDGMENTS

We are grateful to the UK Ministry of Defence for funding via the Defence and Security Accelerator (DSTLX-1000131285).


### REFERENCES


[1] C. L. Evans, and X. S. Xie, “Coherent anti-Stokes Raman scattering microscopy: Chemical imaging for biology and medicine," Annu. Rev. Anal. Chem. 1, 883-909 (2008)

[2] D. Oron, N. Dudovich, and Y. Silberberg, “Femtosecond Phase-and-Polarization Control for Background-Free Coherent Anti-Stokes Raman Spectroscopy," Phys. Rev. Lett. 90, 213902 (2003).

[3] R. Selm, M. Winterhalder, A. Zumbusch, G. Krauss, T. Hanke, A. Sell, and A. Leitenstorfer, “Ultrabroadband background-free coherent anti-Stokes Raman scattering microscopy based on a compact Er:fiber laser system," Opt. Lett. 35, 3282 (2010).

[4] D. L. Marks, C. Vinegoni, J. S. Bredfeldt, and S. A. Boppart, “Interferometric differentiation between resonant coherent anti-Stokes Raman scattering and nonresonant four-wave-mixing processes," Appl. Phys. Lett. 35, 5787 (2004).

[5] N. Dudovich, D. Oron and Y. Silberberg, “Single-pulse coherently controlled nonlinear Raman spectroscopy and microscopy," Science 418, 512 (2002).

[6] F. Ganikhanov, C. L. Evans, B. G. Saar, and X. S. Xie, “High-sensitivity vibrational imaging with frequency modulation coherent anti-Stokes Raman scattering (FM CARS) microscopy," Opt. Lett. 31, 1872 (2006).

[7] C. H. Camp Jr, Y. J. Lee, J. M. Heddleston, C. M. Hartshorn, A. R. Hight Walker, J. N. Rich, J. D. Lathia, and M. T. Cicerone, “High-speed coherent Raman fingerprint imaging of biological tissues," Nature Photonics 8, 627-634 (2014)

[8] D. Pestov, R. K. Murawski, G. O. Ariunbold, X. Wang, M. Zhi, A. V.Sokolov, V. A. Sautenkov, Y. V. Rostovtsev, A. Dogariu, Y. Huang, and M. O. Scully, “Optimizing the laser-pulse configuration for coherent Raman spectroscopy,” Science 316, 265–268 (2007).

[9] D. Pestov, X. Wang, G. O. Ariunbold, R. K. Murawski, V. A. Sautenkov, A. Dogariu, A. V. Sokolov, and M. O. Scully, “Single-shot detection of bacterial endospores via coherent Raman spectroscopy,” Proc. Natl. Acad. Sci. 105, 422–427 (2008).